A Level Set-based Global Shape Prior and Its Application to Image Segmentation

Lei Zhang and Qiang Ji
Rensselaer Polytechnic Institute
110 8th St., Troy, NY 12180
zhangl2@rpi.edu, qji@ecse.rpi.edu

Abstract

Global shape prior knowledge is a special kind of semantic information that can be incorporated into an image segmentation process to handle the difficulties caused by such problems as occlusion, cluttering, noise, and/or low contrast boundaries. In this work, we propose a global shape prior representation and incorporate it into a level set based image segmentation framework. This global shape prior can effectively help remove the cluttered elongate structures and island-like artifacts from the evolving contours. We apply this global shape prior to segmentation of three sequences of Electron Tomography membrane images. The segmentation results are evaluated both quantitatively and qualitatively by visual inspection. Accurate segmentation results are achieved in the testing sequences, which demonstrates the capability of the proposed global shape prior representation.

1. Introduction

Image segmentation is a fundamental and important task in computer vision. Many different kinds of methods have been proposed to solve this problem, including edge-based segmentation [10] [9], region-based segmentation [8] [14], top-down and bottom-up segmentation [3], graph-based segmentation [13], etc. Due to the complexity of image segmentation problems, it is normally not enough to only use the image data for segmentation, especially when occlusion, clutter, noise, and/or low contrast edges exist in the images. Prior knowledge such as the domain knowledge and semantic information are therefore incorporated into the segmentation process in order to improve segmentation results.

Variational method is an important class of segmentation approach. It models image segmentation using an energy functional and converts the problem into a contour evolution process to minimize the energy functional. This approach requires solving the partial differential equation of the energy functional. In recent years, the level set method by Osher and Sethian [15] is extensively used for solving image segmentation problems. Level set method represents an interface implicitly using a surface or hypersurface that is one dimension higher. It can perform numerical computations involving curves and surfaces on a fixed Cartesian grid without having to parameterize them. Moreover, it can easily handle topological changes and can be easily extended to high dimension problems, which make it useful to solve partial differential equations. Researchers have successfully applied level set method into their segmentation framework. Chan *et al*. [4] propose the model of region-based active contours, which can detect objects whose boundaries are not necessarily defined by gradient. Caselles *et al*. [16] propose their segmentation scheme based on the relation between active contours and the computation of geodesics or minimal distance curves. Their scheme segments an image by evolving the active contours according to the intrinsic geometric measures of the image. Rousson *et al*. [12] present a variational framework based on a bayesian model, which utilizes both the image partition information and the statistical parameters of each region.

As mentioned before, pure data-driven image segmentation usually cannot achieve good results when there are such problems of occlusion, noise, cluttering, etc. Incorporation of the semantic information or prior knowledge can help deal with these difficulties. The global shape prior is a specific kind of semantic information that gives the global constraint on the local contours. Many different global shape prior models are proposed in the past few years and incorporated into the level set based image segmentation. Chan *et al*. [5] propose a global shape prior term as the summation of squared differences between the Heaviside functions of the level sets corresponding to the prior shape and the evolving contour. Rousson *et al*. [12] construct the shape prior as the difference between two level set surfaces, which respectively correspond to the reference shape and the evolving contour. Foulonneau *et al*. [2] construct the global shape prior based on affine-invariant moments. Due to the inherent properties of the definition of their shape prior, it is not necessary to estimate the pose of the global reference shape simultaneously with the segmentation. Statistical shape prior is also extensively used to handle varia-

978-1-4244-3993-5/09/$25.00 ©2009 IEEE

tions of the shape prior. Leventon *et al*. [11] incorporate statistical shape prior into Geodesic Active Contours [16] and get the final segmentation using maximum a posteriori (MAP) method. Normally, the statistical shape prior assumes a Gaussian distribution of the prior shape. However, the shape of a real object is usually distorted by nonlinear operation. Cremers *et al*. [6] propose integration of nonlinear shape statistics into a Mumford-Shah based segmentation process [7]. They successfully incorporate into their method the nonlinear prior knowledge on complex real-world shapes.

In practice, we find the extensively used global shape prior [5] has difficulty in segmenting images that contain cluttered elongate structures and island-like artifacts. These reasons motivate us to propose a different global shape prior that can effectively address these problems, which can be useful for segmenting biological images that are usually noisy and have many adjunct structures associated with the main object of interest.

In this paper, we propose a different level set based global shape prior representation based on the contour difference. It can effectively help remove the cluttered elongate structures and island-like artifacts in the evolving contours. We apply the proposed shape prior to segmentation of electron tomography membrane image sequences. Accurate membrane segmentations are achieved and evaluated both quantitatively and qualitatively by visual inspection.

2. Region-based Active Contours

The basic segmentation model used in this paper is similar to the model of active contours [4]. This is a robust model for image segmentation based on piecewise approximation of the well-known Mumford-Shah functional [7]. Instead of using edge detector for stopping the curve evolution, this model uses the region based information (e.g. the intensity) and tries to minimize the summation of intensity variances within the object region and the background region. As a result, it can segment images with low contrast edges along the object boundary. The basic segmentation model is defined by an energy functional

$$\begin{aligned} E(c_1, c_2, C) &= \lambda \int_\Omega |I(x,y) - c_1|^2 H(\phi(x,y)) dxdy \\ &+ \lambda \int_\Omega |I(x,y) - c_2|^2 (1 - H(\phi(x,y))) dxdy \\ &+ \mu \int_\Omega \delta(\phi(x,y)) |\nabla \phi(x,y)| dxdy \end{aligned} \quad (1)$$

where $I(x,y)$ is the intensity at the pixel (x,y). Ω represents the whole image domain. ϕ is the level set function whose zero level set is the evolving contour C. ϕ is selected to be positive for the interior region of C and negative for the exterior region of C. Normally, the interior of the contour C represents the object region and the rest of the image is the background region. $\mu \geq 0$ and $\lambda > 0$ are constant parameters to balance the importance of each term. c_1 and c_2 are the average intensities inside C and outside C, respectively. They can be calculated as follows:

$$c_1(\phi) = \frac{\int_\Omega I \cdot H(\phi) dxdy}{\int_\Omega H(\phi) dxdy};\ c_2(\phi) = \frac{\int_\Omega I \cdot (1 - H(\phi)) dxdy}{\int_\Omega (1 - H(\phi)) dxdy} \quad (2)$$

The function $H(\phi(x,y))$ is the Heaviside function of $\phi(x,y)$ and the function $\delta(\phi(x,y))$ is the one dimensional Dirac function of $\phi(x,y)$. The Heaviside function and the Dirac function are defined as

$$H(z) = \begin{cases} 1, \text{if } z \geq 0; \\ 0, \text{if } z < 0. \end{cases} \quad \delta(z) = \frac{d}{dz} H(z) \quad (3)$$

The first and second terms in Eq.(1) measure the intensity variances of the object and the background, respectively. The third term regularizes the length of the curve C and smooths the curve according to local curvature information. If the image I contains two regions with approximately constant intensities, it can be partitioned into two piecewise constant regions by minimizing the energy functional in Eq.(1). Segmentation is achieved by minimizing the energy functional, i.e.,

$$\inf_{c_1, c_2, C} E(c_1, c_2, C) \quad (4)$$

It can be performed using an iterative process to solve the partial differential equation corresponding to Eq.(1).

Global shape prior information has been incorporated into the segmentation framework of region-based active contours [4]. Chan *et al*. [5] introduce a global shape prior term to impose an additional constraint on the evolving contour C. It restrains the evolving contour to have a similar shape as a global reference shape. Their global shape prior is formulated as

$$E_{shape} = \int_\Omega (H(\phi) - H(\psi))^2 \quad (5)$$

where ψ is the level set function whose zero level set represents the global reference shape. For brevity, we call this shape prior as Chan's prior in the following discussions.

3. The Proposed Global Shape Prior

Chan's global shape prior compares the level set function ϕ with ψ in the whole image domain. It is well known that the level set function ϕ and ψ only depend on the location of their zero level sets. That is, only the zero level sets decide the difference between the evolving contour and the reference shape. We therefore introduce a global shape prior to directly measure the differences between ϕ and ψ only at the zero level set of ϕ, which is defined as

$$E'_{shape} = \int_\Omega (\psi - \phi)^2 |\nabla H(\phi)|^2 = \int_C \psi^2 |\nabla H(\phi)|^2 \quad (6)$$

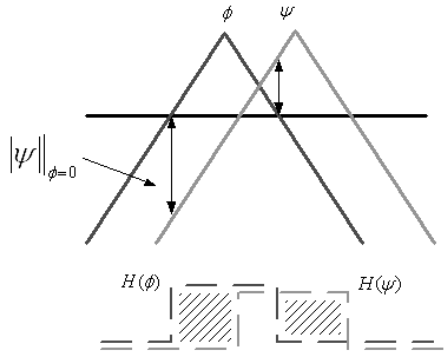

Figure 1. The conceptual difference between the proposed global shape prior and Chan's global shape prior in 1D case

Note that $|\nabla H(\phi)|^2$ is only non-zero on the evolving contour C, where ϕ is zero.

Since $|\nabla H(\phi)|$ is nonzero only at the zero level set of ϕ, this prior term exactly measures the difference between ϕ and ψ at the zero level set of ϕ. We use the squared function for $|\nabla H(\phi)|$ in order to prevent this term from appearing in the denominator of the partial differential equation of Eq.(6). It will avoid instability problem caused by a small denominator that can often happen in a numerical solution. The integral in Eq.(6) is only needed at the zero level set of ϕ, which makes it very easy to implement the more efficient narrow band level set method. This will be valuable for high dimensional problems such as 3D segmentation.

4. The Differences between two Shape Priors

Chan's global shape prior measures the area of the regions where the evolving contour disagrees with the global reference shape. For an image point, if its corresponding values in level set surfaces ϕ and ψ have different signs, then the evolving contour disagrees with the global reference shape at this point. By minimizing this prior term, the level set surface of the evolving contour becomes close to that of the global reference shape. As a result, the evolving contour C will have a similar shape as the global reference shape.

On the other hand, our global shape prior measures the total squared difference between the level sets corresponding to the evolving contour and the global reference shape, only at the zero level set of ϕ. The difference between our prior and Chan's prior is clear. Ours minimizes the difference between two contours while Chan's minimizes the difference between the Heaviside functions of two level set surfaces. The conceptual difference between Chan's prior and ours can be illustrated by Figure 1. In this case, the Chan's prior moves the level set surface ϕ so that the shaded area can be minimized, while our prior moves ϕ so that the differences denoted by the double arrows can be minimized. When the zero level set of ϕ coincides with the zero level set of ψ, both prior terms are zero.

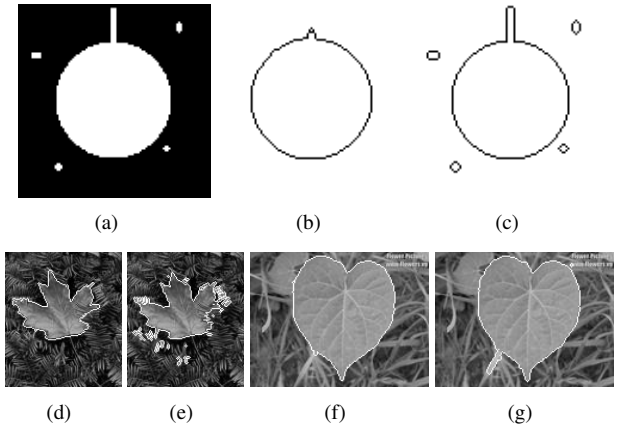

Figure 2. Segmentation results that demonstrate the effectiveness of the proposed global shape prior to remove small island-like artifacts and cluttered elongate structures: a)the synthetic image; b), d) and f) are the produced segmentation results using the model with the proposed prior term; c), e) and g) are the produced segmentation results using the model with Chan's prior.

The concepts of two global shape priors are obviously different, which leads to their different characteristics. Since Chan's prior minimizes the difference between the level set surfaces, it will be insensitive to the small differences on the contours. Our global shape prior focuses on the contours and therefore can pick up the small differences on the contours. For instance, our prior can effectively help remove the cluttered elongate structures and small island-like artifacts. However, the Chan's prior has difficulty in handling such issues. Theoretically, when the evolving contour consists of the reference contour and small island-like artifacts, the "energy" of Chan's prior term is already small because the area of the disagreed regions is small. As a result, this is already a local minimum solution. The optimization process is easily got trapped in the local minimum to produce a sub-optimal solution. Similarly, if the evolving contour consists of elongate structures and the reference contour, the disagreed area encompassed by these elongate structures is also small. The Chan's prior also has difficulty in removing these structures from the final segmentation.

These problems are less significant for the proposed prior. This prior directly measures the difference between two contours. As long as the elongate structures and small island-like artifacts are not too close to the global reference shape, the new prior term is still large, due to the ψ^2 term in Eq.(6). The optimization process will continue evolving the active contour toward a better solution.

Figure 2 shows several segmentation results to demonstrate these characteristics. Both a synthetic image and real images are tested. The synthetic image consists of a circular object, several island-like artifacts and a cluttered elongate structure. The segmentation model using the proposed shape prior term successfully removes most of the island-

like artifacts and the cluttered elongate structure from the segmentation in Figure 2(b). However, the model using Chan's prior has difficulty in removing these artifacts from the final segmentation in Figure 2(c). These artifacts still exist in the final segmentation, even if a very large weight for Chan's prior term is used. Similar phenomena are also observed in the real image segmentations.

5. Segmentation with Global Shape Prior

When the proposed global shape prior is added into the basic segmentation model in Eq.(1), the energy functional corresponding to the segmentation problem becomes

$$\begin{aligned} E(c_1, c_2, C) &= \lambda \int_{\Omega} |I(x,y) - c_1|^2 H(\phi(x,y)) dxdy \\ &+ \lambda \int_{\Omega} |I(x,y) - c_2|^2 (1 - H(\phi(x,y))) dxdy \\ &+ \mu \int_{\Omega} \delta(\phi(x,y)) |\nabla \phi(x,y)| dxdy \\ &+ \gamma \int_{C} \psi^2 |\nabla H(\phi(x,y))|^2 dxdy \end{aligned} \quad (7)$$

where γ is the positive weight of the global shape prior. This functional can be minimized using the corresponding Euler-Lagrange equation as follows:

$$\begin{aligned} \frac{d\phi}{dt} &= -\delta(\phi)\{\lambda[(I-c_1)^2 - (I-c_2)^2] - \mu div(\frac{\nabla\phi}{|\nabla\phi|}) \\ &+\gamma[2\psi^2\delta^{'}(\phi)|\nabla\phi(x,y)|^2 + 4\psi\delta(\phi)\nabla\phi\cdot\nabla\psi \\ &+2\psi^2\delta(\phi)(\phi_{xx}+\phi_{yy})]\} \end{aligned} \quad (8)$$

where ϕ_{xx} and ϕ_{yy} are the second order derivatives of ϕ in column and row directions, respectively. The constant λ is fixed as 2 in all experiments. $\delta^{'}(\phi)$ is the first order derivative of the Dirac function of ϕ. The term $div(\frac{\nabla\phi}{|\nabla\phi|})$ is the curvature term that is normally calculated as

$$div(\frac{\nabla\phi}{|\nabla\phi|}) = \frac{\phi_y^2\phi_{xx} - 2\phi_x\phi_y\phi_{xy} + \phi_x^2\phi_{yy}}{(\phi_x^2+\phi_y^2)^{3/2}} \quad (9)$$

where ϕ_x and ϕ_y are the first order derivatives. ϕ_{xy}, ϕ_{xx} and ϕ_{yy} are the second order derivatives.

In addition, the initial global reference shape may not be in the same pose as the object. It is therefore necessary to estimate a similarity transformation between the global reference shape and the initial reference shape. If ψ is the level set function for the current global reference shape, it is related to the initial reference shape ψ_0 by a four-tuple (a, b, r, θ) [5].

$$\begin{aligned} \psi &= r\psi_0(x^*, y^*) \\ x^* &= \frac{(x-a)\cos(\theta) + (y-b)\sin(\theta)}{r} \\ y^* &= \frac{-(x-a)\sin(\theta) + (y-b)\cos(\theta)}{r} \end{aligned} \quad (10)$$

where (a, b) represents the translation vector. r is the scaling factor and θ is the rotation angle. These parameters shall be estimated simultaneously with the segmentation process. We use gradient descent to estimate them as follows:

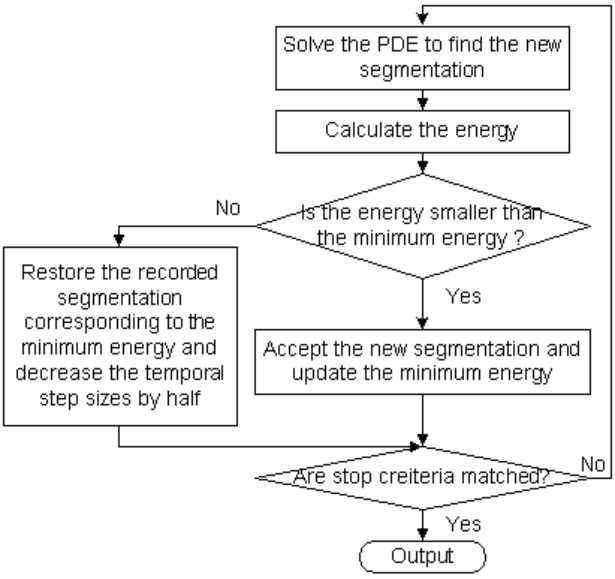

Figure 3. The flowchart of automatically adjusting the temporal step sizes to update the level set function ϕ and (a, b, r, θ).

$$\begin{aligned} \frac{\partial a}{\partial t} &= \int_{\Omega} f(\cdot)\{\psi_{0x}(x^*,y^*)\cos(\theta) - \psi_{0y}(x^*,y^*)\sin(\theta)\}dxdy \\ \frac{\partial b}{\partial t} &= \int_{\Omega} f(\cdot)\{\psi_{0x}(x^*,y^*)\sin(\theta) + \psi_{0y}(x^*,y^*)\cos(\theta)\}dxdy \\ \frac{\partial r}{\partial t} &= \int_{\Omega} f(\cdot)\{-\psi_0(x^*,y^*) + \psi_{0x}(x^*,y^*)x^* \\ &\quad + \psi_{0y}(x^*,y^*)y^*\}dxdy \\ \frac{\partial \theta}{\partial t} &= \int_{\Omega} f(\cdot)\{-r\psi_{0x}(x^*,y^*)y^* + r\psi_{0y}(x^*,y^*)x^*\}dxdy \\ f(\cdot) &= 2\gamma\psi(x,y)|\nabla H(\phi(x,y))|^2 \end{aligned} \quad (11)$$

where ψ_{0x} and ψ_{0y} are the derivatives of ψ_0 in column and row direction, respectively.

The PDE (8) is numerically solved by a two step iterative process. In the first step, we try to roughly estimate a sub-optimal solution. The level set function ϕ corresponding to the evolving contour is updated with a fixed temporal step size. The level set function ϕ corresponding to the minimum energy in this first step is used as the initialization for the second step. The estimated global reference shape ψ corresponding to the minimum energy is also used as the initialization for the second step. In the second step, we automatically adjust the temporal step sizes according to the change of the energy. The flowchart of this process is illustrated in Figure 3. If the energy becomes to increase, we decrease the temporal step sizes in order to find a better solution. If the temporal step sizes are too small or the change of energy is too small, then the iterative process is stopped and the final segmentation is output.

6. Application to Membrane Segmentation

Membrane segmentation is important for medical image analysis. The membrane is a place where many cell activities happen. There are often subcellular assemblies and organelles attached to membranes, which perform cell activities. Knowing the location of membranes can help observe and analyze cell activities. However, membrane segmentation is difficult due to the noise, low contrast membranes, existence of other organelles, cluttered cells, etc.

We applied the segmentation model with the proposed prior on three sequences of different cell images obtained by Electron Tomography (ET). For the first sequence, the goal is to find the membrane of the main cell in all 74 image frames. We manually give a segmentation for every fixed number (e.g. 20) of frames. This manual segmentation is used as the initial global reference shape for the following frames. We use the segmentation of previous frame as the initial contour for the current frame. Each frame is segmented according to the process introduced in Section 5. Two typical segmentation results are shown in Figure 4. By visual inspection, accurate segmentations are achieved.

With the ground truth provided by human experts, we quantitatively evaluate the accuracy of these segmentations. The accuracy of segmentation is measured by the precision and recall rates [1]. Precision is the probability that a machine-generated boundary pixel is a true boundary pixel. Recall is the probability that a true boundary pixel is detected. The average precision and recall values of all segmentations are 92.28% and 99.09%, respectively.

When all segmentations are stacked together, a 3D view of the membranes is established, as shown in Figure 4(c). Although this result is not generated from a 3D segmentation, the wall of the membranes is still smooth, demonstrating the consistency between the segmentations of consecutive frames. In addition, we also segment this image sequence using the level set segmentation with Chan's prior. The 3D view of the stacked membrane segmentations is shown in Figure 4(d). By visual inspection and comparison, the membrane segmentations produced by using our shape prior are smoother than the segmentations produced by using Chan's prior. Besides, there are more adjunct structures incorrectly detected in Figure 4(d).

The second sequence consists of 44 frames. The goal is also to segment the membrane of the main cell in each frame. We use a manual segmentation of the first frame as the initial global reference shape to segment all following frames. A circle is used as the initial contour for segmenting the second image frame. Other frames use the segmentation of their previous frames as the initial contour. Two typical segmentation results are shown in Figure 5. By visual inspection, accurate segmentation is achieved. The average precision and recall values of these segmentations are 99.12% and 97.55%, respectively. Figure 5(c) shows the 3D

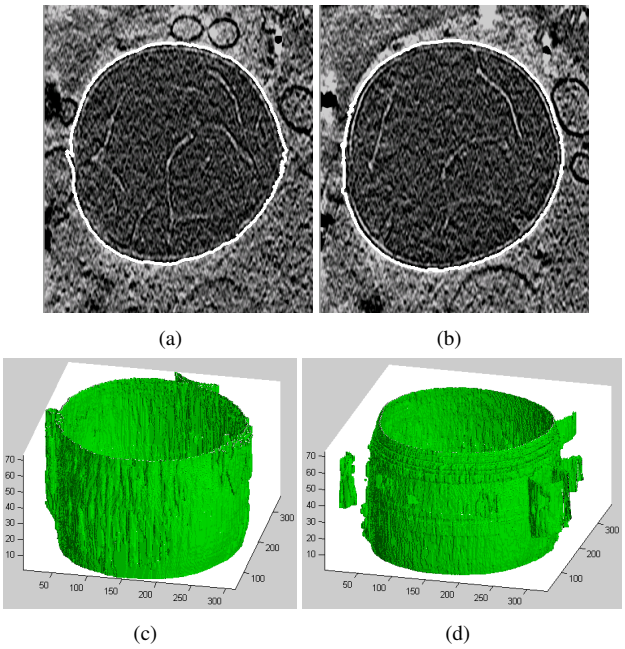

Figure 4. Typical segmentations of two frames (a) and (b) in the first image sequence. The segmentations are superimposed as the white contours on the original images. (c) is the 3D view of the stacked membrane segmentations produced by using our proposed shape prior. (d) is the 3D view of the stacked membrane segmentations produced by using Chan's shape prior.

view of the stacked segmentations of all frames. The wall of the membranes is also smooth, demonstrating the consistency between the segmentations of consecutive frames.

The third sequence consists of cells with two-layer membranes. One is the outer membrane and the other is the inner membrane. The two-layer membrane demonstrates the thickness of a membrane. Our goal is to segment out both the outer membrane and the inner membrane. One key observation is that the inner membrane is roughly a contour shrunk from the outer membrane for a nearly fixed distance. Based on this observation, we first segment out the outer membrane for each frame using a similar process as above. In order to segment out the inner membrane, the segmentation of the outer membrane is shrank by a fixed distance (e.g. 8 pixels). This new contour is used as the initial contour for curve evolution. The inner membrane is then segmented using the same process. Figure 6 shows two typical segmentation results, which visually demonstrate the good accuracy of segmentations. We totally segment out 32 frames and stack all segmentations to generate a 3D view of the membranes, as shown in Figure 6(c). The smoothness of the wall of membranes demonstrates the consistency between the segmentations of consecutive frames.

7. Summary

In this paper, we propose a global shape prior based on contour differences and incorporate it into a level set based

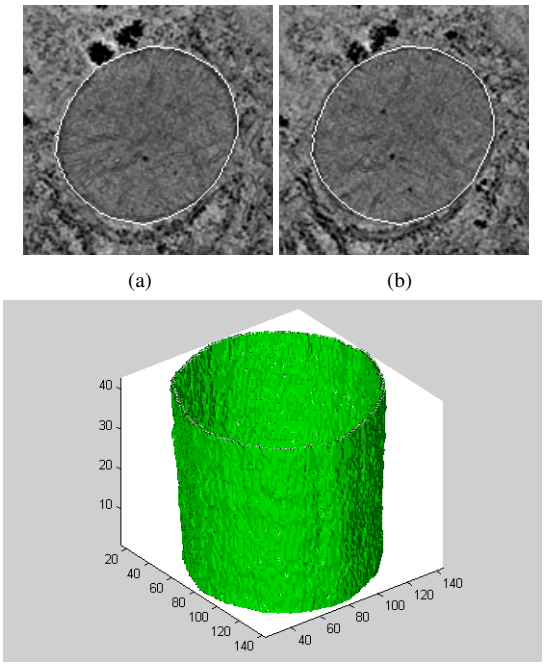

Figure 5. Typical segmentation of two frames (a) and (b) in the second image sequence. The segmentations are superimposed as the white contours on the original images. (c) is the 3D view of the stacked membrane segmentations of the second sequence.

segmentation framework. The proposed global shape prior can effectively remove the cluttered elongate structures and island-like artifacts in the evolving contours. We apply the model with the proposed shape prior to membrane segmentation of image sequences and achieve accurate segmentation results. In the future, we plan to extend this approach to the 3D segmentation problems. Finally, we acknowledge the Wadsworth Center to provide the membrane image sequences for our experiments.

References

[1] Berkeley segmentation dataset and benchmark. http://www.eecs.berkeley.edu/Research/Projects/CS/vision/bsds/.

[2] F. H. A. Foulonneau, P. Charbonnier. Affine-invariant geometric shape priors for region-based active contours, 2006. PAMI, vol.28(8).

[3] J. Borenstein, E. Malik. Shape guided object segmentation, 2006. Computer Vision and Pattern Recognition.

[4] T. Chan and L. Vese. Active contours without edges, 2001. IEEE Trans. Image Processing, vol.10(2), pp. 266–277.

[5] T. Chan and W. Zhu. Level set based shape prior segmentation, 2003. Technical Report 03–66, Computational Applied Mathematics, UCLA, Los Angeles.

[6] T. K. D. Cremers and C. Schnorr. Shape statistics in kernel space for variational image segmentation, 2003. Pattern Recognition, 36(9):1929–1943.

[7] D.Mumford and J.Shah. Optimal approximations of piecewise smooth functions and associated variational problems, 1989. Comm. in Pure and Appl. Math., vol. 42.

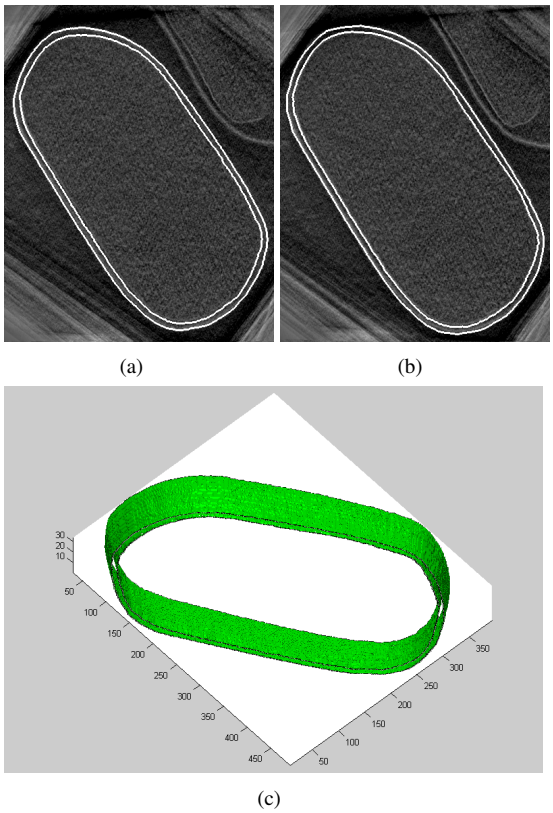

Figure 6. Typical segmentations of two frames (a) and (b) in the sequence of double-membrane cell images. The segmentations are superimposed as the white contours on the original images. (c) is the 3D view of the stacked double-membrane segmentations of the third sequence.

[8] S. S. H L. Jin, A J. Yezzi. Region-based segmentation on evolving surfaces with application to 3d reconstruction of shape and piecewise constant radiance. ECCV 2004.

[9] V. L. Iannizzotto, G. Fast and accurate edge-based segmentation with no contour smoothing in 2-d real images. IEEE Transactions on Image Processing, 2000, 9(7):1232–1237.

[10] C. Leubner. Adaptive color- and edge-based image segmentation using fuzzy techniques, 2001. 7th Fuzzy Days, Dortmund, Lecture Notes in Computer Science.

[11] W. G. M.E. Leventon and O. Faugeras. Statistical shape influence in geodesic active contours, 2000. Computer Vision and Pattern Recognition.

[12] M. Rousson and N. Paragios. Shape priors for level set representations. ECCV 2002, pp.78–92.

[13] J. Shi and J. Malik. Normalized cuts and image segmentation, 1997. IEEE Trans. on PAMI.

[14] F. O. Smarajit Bose. A region-based segmentation method for multichannel image data, 1997. Journal of the American Statistical Association, Vol. 92, No. 437, pp. 92–106.

[15] S.Osher and J.A.Sethian. Fronts propagating with curvature-dependent speed: Algorithms based on hamilton-jacobi formulation, 1988. Journal of Computational Physics, 79.

[16] G. V.Caselles, R.Kimmel. Geodesic active contours, 1997. International Journal of Computer Vision, vol. 22(1).